Density Functional Theory Studies of the Extent of Hole Delocalization in One-Electron Oxidized Adenine and Guanine Base Stacks

ARTICLE *in* THE JOURNAL OF PHYSICAL CHEMISTRY B · MARCH 2011

Impact Factor: 3.3 · DOI: 10.1021/jp200537t · Source: PubMed

2 AUTHORS:

Anil Kumar
Oakland University
59 PUBLICATIONS **1,147** CITATIONS
SEE PROFILE

Michael D Sevilla
Oakland University
222 PUBLICATIONS **6,141** CITATIONS
SEE PROFILE

Published in final edited form as:
J Phys Chem B. 2011 May 5; 115(17): 4990–5000. doi:10.1021/jp200537t.

DFT Studies of the Extent of Hole Delocalization in One-electron Oxidized Adenine and Guanine base Stacks

Anil Kumar and **Michael D. Sevilla**
Department of Chemistry, Oakland University, Rochester, Michigan 48309

Abstract

This study investigates the extent of hole delocalization in one-electron oxidized adenine (A)- and guanine (G)-stacks and shows that new IR vibrational bands are predicted that are characteristic of hole delocalization within A-stacks. The geometries of A-stack (A_i; i = 2 – 8) and G-stack (GG and GGG) in their neutral and one-electron oxidized states were optimized with the bases in a B-DNA conformation using the M06-2X/6-31G* method. The highest occupied molecular orbital (HOMO) is localized on a single adenine in A-stacks and on a single guanine in GG and GGG stacks; located at the 5′-site of the stack. On one-electron oxidation (removal of an electron from the HOMO of the neutral A- and G-stacks) a "hole" is created. Mulliken charge analysis shows that these "holes" are delocalized over 2 – 3 adenine bases in the A-stack. The calculated spin density distribution of $(A_i)^{\bullet+}$ (i = 2 – 8), also, showed delocalization of the hole predominantly on two adenine bases with some delocalization on a neighboring base. For GG and GGG radical cations, the hole was found to be localized on a single G in the stack. The calculated HFCCs of GG and GGG are in good agreement with the experiment. Further, from the vibrational frequency analysis, it was found that IR spectra of neutral and the corresponding one-electron oxidized adenine stacks are quite different. The IR spectra of $(A_2)^{\bullet+}$ has intense IR peaks between 900 – 1500 cm^{-1} which are not present in the neutral A_2 stack. The presence of $(A_2)^{\bullet+}$ in the adenine stack has a characteristic intense peak at ~1100 cm^{-1}. Thus IR and Raman spectroscopy has potential for monitoring the extent of hole delocalization in A stacks.

Keywords

Adenine stack; one-electron oxidized adenine and guanine; vibrational frequency of adenine stack; hole delocalization; hole transfer; ionization potential; nuclear relaxation energy (NRE)

Introduction

The structure and stability of DNA is controlled by many factors among the most important are hydrogen bonding and stacking interactions.[1,2] While the nature of hydrogen bonding between base pairs is well known and extensively studied, the stacking interaction, owing to the difficulty in computing accurate dispersion interactions, is less well investigated by theory.[1–5] In recent years, a number of theoretical methods[4,6] have been developed to describe the structure and properties of stacked molecular systems in their ground and electronic excited states.[7,8] Stacking is of course critical to the migration of holes and

Correspondence to: Michael D. Sevilla.

Supporting Information Available
M06-2X/6-31G* optimized structures of neutral and one-electron oxidized adenine stacks. Spin density plots of A-stacks using UHF and M06-2X. Values of vertical and adiabatic ionization potentials of adenines (A_i, i = 1 – 8) and G-stacks. Optimized structure and plots of spin density distributions of GG and GGG using UHF/6-31+G(d) and M06-2X/6-31+G(d) methods. IR spectra of adenine, A_2 and A_8 in neutral and radical cation states. This material is available free of charge via the Internet at http://pubs.acs.org.

electrons in DNA. Migration of "holes" (positive charge with spin) and excess electrons within DNA take place through the stacked bases in the DNA helix by coupling between the overlapping π-orbitals.[9–14] This charge carrier property of the DNA has received enormous research interest in many areas which explore its role in biological cellular process and its use in DNA-based electrochemical devices.[9–22] One-electron oxidation and reduction processes are the primary steps in DNA radiation damage. Thus nature of charge migration in DNA has important implications to ultimate localization of DNA damage. [9–14]

The mechanism of long distance charge transfer along the DNA strand has been examined extensively by experiments and supplemented by theoretical studies.[19–30] There are several factors, such as, coupling, structure and dynamics of the DNA assembly, which affect the charge transfer in DNA.[19,25c] The experiments of Giese and coworkers[30] showed the important role of adenines as "hole" carrier in the sequences of $G(A:T)_nGGG$, where n = number of intervening A:T base pairs between G donor and GGG as acceptor. These experiments proposed two distinct types of mechanisms for charge transfer from G to GGG through intervening adenines that are present in the sequences: (i) Superexchange charge transfer (tunneling) in the short sequences $G(A:T)_{n=1–3}GGG$ and (ii) Thermally induced hopping of charges between stacked adenines in the long sequences $G(A:T)_{n>3}GGG$. However, Barton and coworkers19c presented experimental evidence that hole wavefunctions were delocalized over several adenine bases in DNA. Using femtosecond broadband pump-probe spectroscopy, Fiebig and coworkers[31] showed that in $(dA)_n$ (dA is 2′-deoxyadenosine) and $(dA)_n•(dT)_n$ the transition wavefunction is delocalized over 3 – 4 bases. Conwell and coworkers[29] proposed that these delocalized states can be transported by polaron, which are delocalizing up to 2 – 5 adjacent bases in DNA, depending on the DNA sequence. The formation of delocalized states are, also, supported from molecular dynamics simulation and quantum chemical calculations.[7,8,25,28,32,33] In a very recent study, using ESR spectroscopy and theory, the hole delocalization on two adenine bases in one-electron oxidized stacked DNA-oligomer $(dA)_6$ was confirmed.[34] The stability of $(A_2)^{•+}$ in $(dA)_6$ was explained by the formation of a delocalized charge resonance state. Very recently, Majima and coworkers[35] observed charge resonance bands in p-stacked multi-benzene rings in multilayered para- and meta-cyclophanes. These charge resonance bands arise due to delocalization of positive charge in the π-stacked-benzene rings. The study was carried out using transient absorption spectroscopy and pulse radiolysis experiments. For the stacks of other DNA bases no such delocalization of "hole" has been found experimentally. Theory shows that on nuclear relaxation "hole" localizes more strongly at one guanine base in guanine-guanine (GG) stack than for AA stack.[33] This finding is also supported from a recent ESR study[36a] which showed that in a GGG sequence the hole is localized on one guanine at 77 K.

From previous work,[34] it is evident that stacked adenines play a unique role in hole transfer within DNA as there is good experimental evidence that holes in stacked adenines are delocalized in nature. To further elucidate this interesting property of adenine stacks as long range charge carriers in DNA, in this work, we study the stacks of adenines ranging from dimer to octamer in a B-DNA conformation. We also considered the GG and GGG stacks in their neutral and radical cation states as these are known to be the efficient hole traps (with the hole localized on one guanine base) owing to their decreasing ionization potentials with stack length.[20,30b,33,36] Our results shed light on: (i) The nature of HOMO and spin localization in neutral and one-electron oxidized adenine and guanine stacks. (ii) The variation of ionization potential with increasing length of the adenine and guanine stacks. (iii) The degree of hole delocalization in one-electron oxidized adenine and guanine stacks. Finally, (iv) Characteristic IR bands of $A_2^{•+}$ are predicted that would allow for the identification of charge delocalization in adenine stacks.

Method of calculations

The geometries of adenine stacks ranging from dimer to octamer were optimized in the B-DNA conformation using the M06-2X density functional developed by Truhlar and Zhao.[6] The M06-2X functional is a hybrid meta GGA (generalized gradient approximations) functional having 54% Hartree-Fock exchange contribution.[6] Because of the large Hartree-Fock exchange contribution, this functional is a better choice than other functionals e.g. B3LYP which is severely affected by the self-interaction error.[6f] This newly developed M06-2X functional has been found very suitable for studying a number of chemical problems including molecules having radical character[6e] and especially shows its wide applicability to the study of non-covalent interactions. In the present calculation, the initial starting geometries of adenine stacks ranging from $A_2 – A_8$, GG and GGG in B-DNA conformation were generated using Spartan molecular modeling program.[37] From the generated structures in B-DNA conformation, we removed the sugar, phosphate backbone attached to the bases and neutralized the N_9 site of each base in the stack with hydrogen atom; the initial structure thus generated retains the B-DNA base conformation and is abbreviated as “B-DNA conformation” in the text. Since we are dealing with large stacks that require considerable CPU time and since the calculations scale with the size of the basis set, we used 6-31G* basis set for geometry optimization to make these calculations feasible. We also calculated the spin density distributions with 6-31+G* and 6-31++G** basis sets for the cationic adenine stacks to observe the extent of hole delocalization within the stack. The geometries of (A_i) (i = 2 – 8), GG and GGG thus generated were used to optimize the structures in their neutral state using the M06-2X/6-31G* method. During geometry optimization only the mutual orientation of the stacked bases were constrained to retain the B-DNA conformation while all the intramolecular degrees of freedom and the inter-base distances between the bases in the stack were fully relaxed. In our constrained geometry optimization criterion, we constrained two dihedral angles $N_{7a}N_{7b}N_{9b}N_{9a}$ and $N_{3a}N_{3b}C_{6b}C_{6a}$ and angles $N_{7a}N_{7b}N_{9b}$, $N_{7b}N_{9b}N_{9a}$, $N_{3a}N_{3b}C_{6b}$ and $N_{3b}C_{6b}C_{6a}$ between two adjacent bases a and b present at the one of the end in the stack and applied the same criteria to each successive base in the stack, see Figure 1 for atom numbering. A detailed description is given in our earlier work.[33a] Using the same method and geometry optimization criterion; the optimized geometries of the neutral stacks (A_i, i = 2 – 8) were used as input for optimizing the corresponding stacks in their radical cation (one-electron oxidized) states. All the calculations were performed using Gaussian 09 suite of programs.[38] GaussView molecular modeling software[39a] was used to plot the molecular orbitals and drawing the molecular structure. The Gabedit molecular modeling package was used to plot vibrational spectra.[39b]

Results and Discussion

Suitability of the M06-2X Functional

Before performing the actual calculations, it is important that the suitability of the M06-2X method to treat problems that involve stacked radical cations be established. It is well known that DFT functionals suffer from the self-interaction error (SIE) and can show excess delocalization of hole (positive charge) in stacked systems. Using B3LYP and BLYP functionals Close[40] and Mantz *et al*.[41] found hole delocalization on one-electron oxidized purines and questioned the applicability of the DFT method to such type of problems. This shortcoming of the DFT method can be remedied either by applying an empirical correction scheme to the functional, e.g., BLYP, as proposed by VandeVondele and Sprik[36, 42] or by increasing the Hartree-Fock exchange (HFX) contribution in the functional; a number of recent publications have appeared in the literature which show the effectiveness of this latter approach.[43] Mantz *et al*.[41] found that SIE corrected BLYP functional localized the hole appropriately but it grossly errored in the ordering of the ionization potentials of the DNA

bases. An excellent very recent work by Guidon, Hutter and VandeVondele[43a] shows the degree of localization of spin density of a single hole in a cluster of 64 water molecules as a function of the fraction of Hartree-Fock exchange employed in the PBE0 functional. The result clearly demonstrates that functionals containing 50 – 60 % HFX appropriately localizes the spin density, see Figure 2 of reference.[43a] Also, an assessment of the performance of M06-2X method (54% HFX) for non-covalent interactions in biomolecules has been performed by Sherrill and coworkers[44] using JSCH-2005 database. Using the CCSC(T) binding energies as benchmark; the M06-2X method was found to accurately treat stacked base pairs.[44] Gu *et al.*[45] demonstrated that the M06-2X functional predicts structures of stacked DNA bases similar to those obtained by MP2 and the calculated stacking energies were in good agreement with those calculated using the CCSD(T) level of theory. In addition, in the present work, we used the unrestricted Hartree-Fock (UHF) method and plotted the spin densities of adenine stacks to test the suitability of the M06-2X functional for these systems. For radical cations, the UHF method is widely used as a reference.[41, 43a] We also used 6-31+G* basis set to see the effect of basis set on the hole delocalization in the radical cation of adenine stacks ($A_2 – A_8$) and used even larger basis set 6-31++G** for $A_8^{\bullet+}$. Finally, we compare the nature of "hole" delocalization in two different types of DNA stacks (A- and G-stacks). These calculations for A- and G-stacks show that the "hole" is delocalized on A-stacks and localized on G-stacks.

Adenine and Guanine Stacks

The M06-2X/6-31G* optimized structures of octamer adenine stack (A_8) in neutral and radical cation states along with the atom numbering scheme for adenine and guanine are shown in Figure 1. Each individual adenine base present in the stack is numbered as $a_1 – a_8$, see Figure 1(b, c) for A_8 and Figure S1 (in the supporting information) for $A_2 – A_7$. The optimized structures of neutral and radical cation of A_i (i = 2 – 7) are presented in the supporting information as Figure S1. In Figure 2, we present the plots of the HOMOs of the neutral A stacks and the spin density distribution of the radical cation of A stacks, i.e., A_i (i = 2 – 8). In Figure 3, we present the plots of spin density distributions and HOMOs of GG and GGG. The variation of the vertical and adiabatic ionization potentials (IP) in electron volt (eV) with the increase of the stack length is shown in Figure 4.

Structure of Adenine Stacks

The inter-base geometrical parameters between the bases in A_8, optimized in the B-DNA conformation (structure shown in Figure 1) by M06-2X/6-31G* level of theory, are presented in Table 1. In Table 1, the inter-atomic distances between the corresponding atoms of two consecutive adenine bases chosen as a_1-a_2, a_2-a_3, a_3-a_4, a_4-a_5, a_5-a_6, a_6-a_7 and a_7-a_8 in the A_8 stack are given. For example, we chose N_1, C_2, N_3, C_4, C_5, C_6, N_6, N_7, C_8 and N_9 atoms of one of the adenine (a_1) and calculated the inter-atomic distances between the corresponding atoms of the other adenine a_2, the two adenines a_1 and a_2 thus chosen are designated as a_1-a_2 in Table 1, see Figure 1a for numbering of adenine bases in the stack. From Table 1, we see that in neutral state of A_8 the distances between N_1 atoms lie between 3.17 – 3.21 Å, C_2 atoms 3.41 – 3.44 Å, N_3 atoms 3.70 – 3.74 Å, C_4 atoms 3.72 – 3.75 Å, C_5 atoms 3.53 – 3.56 Å, C_6 atoms 3.22 – 3.26 Å, N_6 atoms 3.25 – 3.29 Å, N_7 atoms 3.89 – 3.91 Å, C_8 atoms 4.20 – 4.25 Å and N_9 atoms 4.16 – 4.18 Å, respectively. The average distance for N_1, C_2, N_3, C_4, C_5, C_6, N_6, N_7, C_8 and N_9 atoms are 3.19, 3.43, 3.72, 3.73, 3.54, 3.24, 3.26, 3.90, 4.23 and 4.17 Å, respectively, see Table 1. From these distances, it is evident that adenines in the neutral A_8 stack are situated roughly equidistant from each other. The inter-base distances between two adenines in the neutral A_8 stack are also calculated from the location of the geometrical center calculated for each adenine in the stack and the distances lie between 3.463 Å to 3.490 Å, respectively. For cationic A_8 stack the inter-base distances lie between 3.445 Å to 3.505 Å, see Figure S13. The X-ray crystallographic structure of 5′-

d(CpGpCpGpApApTpTpCpGpCpG)-3′ dodecamer in B-DNA conformation (PDB code: 1BNA.pdb) has been determined by Drew *et al.*[46] From this structure, we measured the corresponding distances between the two consecutive adenine bases, present at 5^{th} and 6^{th} positions at the both strand, and the distances for N_1 atoms are 3.47, 3.43 Å, C_2 atoms 3.72, 3.7 Å, N_3 atoms 3.94, 4.01 Å, C_4 atoms 3.82, 4.01 Å, C_5 atoms 3.58, 3.79 Å, C_6 atoms 3.39, 3.47 Å, N_6 atoms 3.49, 3.48 Å, N_7 atoms 3.87, 4.14 Å, C_8 atoms 4.25, 4.51 Å and N_9 atoms 4.25, 4.47 Å. The NMR solution structure of a DNA dodecamer d(GGCAAAAAACGG) containing an A-tract (six adenines; PDB code: 1FZX.pdb) has been determined by MacDonald *et al.*[47] The average distances for N_1, C_2, N_3, C_4, C_5, C_6, N_6, N_7, C_8 and N_9 atoms between the two adjacent adenines are 3.32, 3.68, 3.98, 3.88, 3.54, 3.23, 3.18, 3.87, 4.30 4.36 Å, respectively, see Table 1. A comparison between M06-2X/6-31G* calculated inter-atomic distances and the experimental crystallographic and NMR values show that our theoretical values are underestimated by 0.1 – 0.3 Å. This difference is not surprising since the X-ray and NMR structure includes the effect of solvation of the surrounding waters, hydrogen-bonding between the base pairs and thermal effects, which are not included in the present calculation. The NH_2 group in each adenine in the stack acquires non-planarity and this is because in the calculation the effect of hydrogen bonding is missing; it is not unusual and has been reported in several studies.[1i, j]

For radical cation of A_8 stack, the corresponding inter-atomic distances between the bases are similar to those calculated for the neutral state except for second and third adenines (a_2 and a_3) in the stack, for which the distances between them were decreased by ~ 0.1 Å, see Table 1. It shows that on one-electron oxidation the electronic coupling between the a_2 and a_3 adenines is enhanced and as a consequence they are pulled closer together. Strong electronic coupling between bases is critical to efficient hole/electron transfer in DNA, as pointed out by Voityuk *et al.*[25] and others[26–29] in a number of publications.

Nature of orbital localization

(a) Adenine stacks

Plots of the HOMOs for the optimized adenine stacks (A_i; i = 2 – 8) in their neutral state along with the spin density plots of the corresponding optimized adenine stacks (A_i; i = 2 – 8) in their radical cation state are shown in Figure 2. Our calculations, using the M06-2X/6-31G* level of theory, show that in neutral state the HOMO in all the considered adenine stacks (A_i; i = 2 – 8) is localized predominantly on one adenine base located at one of the ends of the stack, see Figure 2. Recently, the ground and excited states of π-stacked 9-methyladenine oligomers was studied by Improta.[7a] The ground state geometry optimization of π-stacked 9-methyladenine pentamer was performed in aqueous solution at the PCM/PBE0/6-31G(d) level of theory. The calculation showed the delocalization of HOMO on three adenines in the pentamer of 9-methyladenine, located in the middle of the stack. This difference might be due to the difference in imposing the different geometry optimization criterion. In our calculation, we only constrained the mutual orientations between the bases in the stacks while Improta,[7a] in his calculation, constrained the mutual orientation and inter-base distances between the bases in the stack.

A radical cation (hole) in an adenine stack is produced by the removal of one electron from the neutral adenine stack. Spin density plots, shown in Figure 2, provide information about the nature of the hole localization in the optimized radical cation adenine stack. From Figure 2, we found that spin densities in $(A_i)^{\bullet+}$; (i = 2 – 8) are delocalized mainly on two adenines a_2 and a_3 (see Figure 1c for numbering) with some spin delocalization on the neighboring bases a_1 and a_4, see Figure 2. The localization of spin density on two adenines (a_2 and a_3) correlates with the reduced inter-base distance between them in comparison to the other adenine bases in the stack, see Table 1. The reduction in the inter-base distance in the radical

cation state increases the electronic coupling between a_2 and a_3 as reported by Voityuk *et al.* 25c. Our calculations are further supported by a recent work employing ESR experiment and theory, in which, the delocalizing the hole on two adenines, i.e. $(A_2)^{\bullet+}$, in one-electron oxidized stacked $(dA)_6$, was proposed.[34] The stability of $(A_2)^{\bullet+}$ in $(dA)_6$ was proposed to be due to charge resonance interactions. The delocalized nature of hole on stacked $A_2^{\bullet+}$ was also supported form the CASSCF/CAS-PT2 level of theory by Voityuk *et al.*[25,33b], DFT calculations[33a] and equation-of-motion coupled-cluster method with single and double substitutions (EOM-CCSD) by Krylov *et al.*[48]

Further, we calculated the spin densities for the cationic adenine stacks using the UHF/6-31G* method considering the M06-2X/6-31G* optimized geometries. UHF is used as a reference for such type of problems,[41, 43a] especially for radical cations because UHF does not show self-exchange interactions at long range. The plots of the UHF/6-31G* spin densities are shown in the supporting information as Figure S2. Form the UHF/6-31G* spin density plots, it is evident that spin densities are delocalized within the adenine stack as obtained by M06-2X/6-31G* method. In fact, UHF-calculated spin densities are slightly more delocalized on three adenine bases in the adenine stack than the M06-2X calculated spin densities, see Figures 2 and S2. Spin densities calculated at the M06-2X/6-31+G* level of theory for $(A_2^{\bullet+} - A_8^{\bullet+})$ and M06-2X/6-31++G** level of theory for $A_8^{\bullet+}$ are shown in Figures S2 and S3 in the supporting information. From the spin density plots, calculated using M06-2X method and 6-31G*, 6-31+G* and 6-31++G** basis sets (see Figures 2, S2 and S3), we see that the nature and the extent of the spin density distribution are similar for each of these basis sets.

In Table 2, we present the charge distribution on each individual adenine in the stack, see Figures 1 and S1 (in the supporting information) for numbering of the adenine base in the stack. The total charge on each adenine was calculated from the sum of the Mulliken atomic charge on each individual adenine base in the stack. Table 2 shows that in the neutral state each adenine maintains an almost neutral state as expected. The terminal adenine a_1 in the stack gains a little charge ~ −0.01e (e is electronic charge). In radical cation state, the positive charge (hole) distribution is calculated as the difference between the total charges on individual adenine present in the radical cation stack to the corresponding adenine present in the neutral stack as used by Drew *et al.*[49] As can be readily seen from Table 2, the positive charge (hole) is delocalized over 3 – 4 adenines in the stack and largely localized on the second adenine in the stack. Our calculations show that spin and hole distribution follow each other as expected.

(b) GG and GGG stacks

Guanine stacks pose both interesting and challenging problems for testing the applicability of the theoretical methods especially DFT. Many experiments show that GG and GGG stacks act as a hole trap.[20,30b,36] On one-electron oxidation of GG or GGG hole localizes on one guanine preferentially at the 5′-site in the DNA.[50,51] The radical cation of GG stack has been studied by Close[40] and Mantz *et al.*[41] using UHF/6-31+G(d), B3LYP/6-31+G(d), ROHF, CASSCF, ROBLYP and self-interaction corrected ROBLYP (ROBLYP-SIC) methods by placing GG stack in a parallel conformation for maximizing the overlap between the orbitals. It is noted that these conformations are not pertinent to the actual DNA conformation. We also carried out an extensive study considering the parallel GG stack (for maximum overlap) in C_s and C_1 symmetries using UHF/6-31+G(d) and M06-2X/6-31+G(d) level of theories. We found spin delocalization to both bases in the GG stack for both the methods (UHF and DFT) in both symmetries, i.e., C_s and C_1 symmetry which has maximum base-to-base overlap. For details of the calculations see the supporting information and Figures S4a, b. However, on the breaking of molecular symmetry and allowing lateral motion of the bases (slipping), the structure optimized to a state which has localized spin on

one guanine (> 97%) in GG, see Figure S4b (below the line) in the supporting information. Also, this structure is about 7 kcal/mol more stable than the corresponding parallel GG structure in C_1 symmetry showing that delocalized holes in GG are higher in energy than the localized state.

The neutral and radical cation states of GG and GGG in the B-DNA conformation were optimized using the M06-2X/6-31G* method and plots of spin density distribution of radical cations and HOMO of neutrals are shown in Figure 3. For GG and GGG radical cations, we see that spin densities (> 90 %) are localized on one guanine, which clearly supports the experimental observations.[20,30b,36] Our M06-2X/6-31G* calculations are also supported by the high level of calculations using CASSCF and CASPT2 by Blancafort and Voityuk[33b]. We, also, found that the HOMOs of neutral GG and GGG are localized on one guanine, see Figure 3. The M06-2X/6-31G* calculated isotropic hyperfine coupling constants (HFCCs) in MH_z of G, GG and GGG along with experimental HFCCs values, obtained from ESR experiment for DNA[36, 52] and single crystal[40], are presented in Table 3 and in Tables T1 and T2 in the supporting information. In GG and GGG the calculated HFCCs are predominantly localized only on one guanine base and are substantially localized at N_3, NH_2', NH_2'' and C_8-H atoms The calculated HFCCs are in good agreement with the corresponding experimental ESR HFCCs values, see Table 3. The C_8-H coupling calculated for G, GG and GGG are −22.43 MHz −20.84 MHz and −19.63 MHz, respectively. These calculated C_8-H couplings are in very good agreement with the ESR experimental value of 22.6 MHz or ~8 Gauss.[36,52]

Ionization potential

The ionization potential (IP) of DNA bases is an important quantity that provides information about the primary oxidation energy in DNA systems. The ionization potential of DNA bases has been studied extensively using theory and experiment.[11,12] The variation of vertical and adiabatic ionization potential of A_i, i = 1 – 8, calculated by the M06-2X/6-31G* method, is shown in Figure 4. The calculated vertical and adiabatic ionization potentials of a single adenine, 8.32 and 8.04 eV, are in close agreement with the corresponding experimental[53a,b] values 8.44 and 8.26 eV, respectively, see Table T3 in the supporting information. Our M06-2X/6-31G* calculated IP values of A_2 8.02 eV (vertical) and 7.67 eV (adiabatic) are also in very good agreement with those calculated using EOM-IP-CCSD/ 6-311+G(d,p) method and the corresponding values are 8.16 eV (vertical) and 7.57 eV (adiabatic), respectively.[48] From Figure 4, it is evident that IP of adenine stacks decreases with increase in the stack length. The decrease in the IP is pronounced for up to 4 adenines (~0.7 eV) and after that the decrease in the IP is moderate, i.e., ~0.3 eV (vertical) and ~0.1 eV (adiabatic), see Figure 4 and Table T3. The difference between vertical and the adiabatic IPs gives nuclear relaxation energy (NRE). Our calculated NRE values for A_i, i = 2 – 8 vary between 0.2 eV to 0.4 eV. Compared to the experimental NRE value of adenine ~0.2 eV; our calculated NRE value for adenine is slightly overestimated by 0.1 eV, see Table T3. From Table T3, it is seen that for A, A_2 and A_3, NRE value increases from 0.28 eV to 0.39 eV and there after it decreases and attains the value 0.2 eV for A_8. After correcting the M06-2X/6-31G* calculated NRE values for A_i, i = 1 – 8 by 0.1 eV, the corresponding NRE values likely lie in the range 0.1 – 0.3 eV. In an earlier study[53c] the NRE value of adenine in AT base pair was calculated as 0.1 eV at the B3LYP/6-31+G(d) level of theory. A small value of NRE for adenine suggests that geometry of one-electron oxidized adenines in AT stacks would not be significantly different than the corresponding geometry of the adenines in the neutral stack and would clearly aid hole delocalization and hole transfer through A stacks.

The M06-2X/6-31G* calculated vertical and adiabatic ionization potentials of G, GG and GGG are presented in Table T4 in the supporting information. The variation of IP with number of Gs is shown in Figure 4. From Figure 4, it is evident that every G-stack has a lower ionization potential than the corresponding adenine stack. The M06-2X/6-31G* calculated vertical and adiabatic IPs (8.03 eV and 7.58 eV) of G are in good agreement with the corresponding experimental values (8.24 eV and 7.77 eV).[53a,b] An improved agreement with experiment is obtained with 6-31+G(d) basis set having a maximum difference of 0.06 eV, see Table T4. The vertical and adiabatic IPs of GG and GGG are 7.47 eV and 7.03 eV (vertical) and 7.19 eV and 6.76 eV (adiabatic), see Table T4. The NRE value (0.45 eV) in G-stack is larger than the A-stack (0.1 – 0.3 eV). The large NRE value (0.45 eV of G-stacks) shows that on one-electron oxidation a large change in the geometry of G-stacks is expected than the neutral G-stack. Clearly no stack of A will have a lower IP than a G stacked system. It is also noted that the NRE calculated above is directly related to the inner-sphere reorganization energy ($_{i,A}$) appeared in the Marcus theory, see Table 2 in Ref. 53g. This quantity is a critical determinant of the rate of charge transfer.[28b, 53d–f]

Vibrational analysis

IR and time resolved resonance Raman spectroscopies are excellent diagnostic tools for structure identification of molecules that are sensitive to the oxidation state of the molecule.[54] Using the M06-2X/6-31G* optimized geometries of neutral and one-electron oxidized adenine monomer and A_2 we performed a vibrational analyses for these structures. For $A_2^{\bullet+}$ and A_2 (constrained B-DNA conformation), as would be expected, we found very small negative frequencies, for $A_2^{\bullet+}$ (−35 cm^{-1} and −5 cm^{-1}) and for A_2 (−19 cm^{-1}). Thus, considering the M06-2X/6-31G* constained optimized structures of $A_2^{\bullet+}$ and A_2, we fully optimized the geometries of $A_2^{\bullet+}$ and A_2 at the same level of theory. The fully optimized geometries of radical cation and neutral A_2 along with their spin density and HOMO plots are shown in Figure 5. The fully optimized structures are stabilized by 0.21 eV ($A_2^{\bullet+}$) and 0.1 eV (A_2) than their corresponding structure optimized in the B-DNA conformation shown in Figure S1. The fully optimized structures (shown in Figure 5) have all positive frequencies shown in Figure 6. The spin densities on $A_2^{\bullet+}$ are found to be delocalized on both the adenines in the ratio 63% and 37% while the HOMO is predominantly localized on a single adenine base in A_2, see Figure 5. The vibrational spectra of fully optimized A, $A^{\bullet+}$, A_2 and $A_2^{\bullet+}$ are shown in Figures S8 – S11 in the supporting information and in Figure 6(A_2 and $A_2^{\bullet+}$), respectively. The vibrational spectra of A and $A^{\bullet+}$ are described in the supporting information.

In going from monomer to dimer a large change in the vibrational spectra of $A_2^{\bullet+}$ is observed, see Figure 6. For A_2, the most intense peak is located at 1712 cm^{-1}. The infrared spectra are assigned by the visual inspection of the atomic displacement along the normal modes of the molecule. Between 3200 cm^{-1} to 3700 cm^{-1}, the weak peaks are assigned as stretching mode of C_2-H, C_8-H, NH_2 (symmetric), N_9-H and NH_2 (antisymmetric) as observed for monomer. A medium intense peak at 614 cm^{-1} is assigned as NH_2 wagging mode. The vibrational spectra of $A_2^{\bullet+}$ is significantly different than A_2 and between 800 cm^{-1} – 1600 cm^{-1} intense peaks are observed. The most intense peak is located at 1098 cm^{-1} which is not present in the corresponding neutral state of A_2. Two intense peaks, almost of equal intensity, are located at 1218 cm^{-1} and 1372 cm^{-1}. Thus, our calculations show that in one-electron oxidized stacked adenine, dimer radical cation ($A_2^{\bullet+}$) is formed, which has a characteristic frequency ~1100 cm-1 and shows new peaks between 1000 cm^{-1} to 1600 cm^{-1}. In this context, we note that recently Parker *et al.*[54a,b] characterized the formation of guanine radical cation in the infrared region by ionizing DNA in rigid aqueous glasses at 77 K with 193 nm laser. Tripathi *et al.*[54c–f] has successfully employed resonance

Raman spectroscopy to identify radical cations in time resolved studies which suggests its possible applicability to cation radicals of adenine stack.

We also note that A_2 and $A_2^{\bullet+}$ optimized in the B-DNA conformation (structures shown in Figure S1) have small negative vibrational frequencies (discussed above) the vibrational spectra is shown in Figure S12 in the supporting information. The computed IR spectra of $A_8^{\bullet+}$ and A_8 in the B-DNA conformation also have small negative frequencies (−52 cm^{-1} and −36 cm^{-1}; $A_8^{\bullet+}$) and (−26 cm^{-1} to −7 cm^{-1} (total 7); A_8), see Figure S12. This is a normal consequence of geometries optimized under constraints, i.e., in this case the B-DNA conformation. Imposing constraints on a structure to retain a specific conformation or symmetry usually results in small negative frequencies as reported by Smith and Gordon[55] for the calculation of neutral and anionic clusters of Al_{13}. Though these (A_2, $A_2^{\bullet+}$, A_8 and $A_8^{\bullet+}$) have small negative frequencies, the overall features of these spectra are similar to those computed with fully optimized A_2 and $A_2^{\bullet+}$, see Figures 6 and S12. $A_2^{\bullet+}$ and $A_8^{\bullet+}$ have intense peak at near 1100 cm^{-1} and a number of other peak not found in the neutral stacks in the range 900 cm^{-1} to 1500 cm^{-1} just as found for the fully optimized $A_2^{\bullet+}$. From the visual inspection of the vibrations of the various normal modes of $A_8^{\bullet+}$, it is clear that particular modes of vibration, such as, ring breathing modes of each adenine in the stack are coupled with each other in the range 735 – 744 cm^{-1}. It has been proposed by a variety of workers that thermally induced vibrational dynamics of the bases in DNA, as well as, counter ion and solvent dynamics would mediate charge transfer processes in DNA. Our work adds support to researchers who have, also, suggested that the formation of transient delocalized domains in A stacks in DNA combined with the above mention DNA dynamics would enhance such transfer. [26, 29, 56–58]

Conclusions

From the present study, we find that DFT using the M06-2X/6-31G* method predicts structures of neutral adenine stacks ranging from A_2 – A_8 in the B-DNA conformation that are in reasonable agreement with a B-DNA structure (PDB code: 1BNA.pdb and 1FZX.pdb)[46,47] but with slightly lower base-to-base separations. The optimized structures of one-electron oxidized adenine stacks ($A_2^{\bullet+}$ to $A_8^{\bullet+}$) show interatomic distances similar to those calculated for the neutral state except for the two adenines where the hole is localized, i.e., a_2 and a_3 (see Figure 1) for which the inter-atomic distance between them is reduced by ~ 0.1 Å, see Table 1. This decrease in the inter-base distance is a result of increased electronic coupling between them.[25 – 29]

For the stacks of A_2 – A_8, the highest occupied molecular orbital is localized at a single adenine base at one of the end of the stack. On one-electron oxidation of the neutral adenine stacks, a hole is created in the stack which shows a delocalized nature. The Mulliken charge distribution shows the delocalization of positive charge (hole) on 2 – 3 adenines in the stack. This delocalization of hole in adenine stacks is further supported from spin density calculations, which shows that hole is mainly delocalized on two adenines in the stack with very small distribution of spin on the neighboring bases in the stack. The spin distribution in the stack indicates the presence of adenine dimer radical cation in the stack as observed by ESR experiment.[34] This delocalized nature of hole distribution is supported from several experimental and theoretical efforts.[7,8,26,28,29,33,48,55 – 57] These calculations were done for gas phase systems and lack the environmental effects such as hydrogen bonding and solvent induced polarization which further affect the hole delocalization in A-stacks. However, our earlier study[34] on adenine dimer radical cation in the presence of several water molecules showed that spins were still delocalized in the ratio 73% and 27%.

The radical cations of GG and GGG stacks behave very differently from those of A-stacks. The plotted spin density distributions are localized on single guanine base in GG and GGG stack. The plotted HOMOs of GG and GGG also show the localized nature as observed experimentally.[20,30b,36] The calculated HFCCs of GG and GGG stacks matched very well with experimental HFCCs.[36,40, 52]

The M06-2X/6-31G* calculated ionization potential of adenine stacks shows an expected lowering of the IP with the increase of the stack length. The decrease in the IPs is largest for the first four adenines in the stack and decrease as the stacks increase in size. The M06-2X/6-31G* calculated vertical and adiabatic IPs of adenine monomer and dimer are in very good agreement with the available experimental values and high level theoretical calculations using EOM-IP-CCSD/6-311+G(d,p) method.[48] The lowering of the IP with the size of the adenine stacks as well as hole sharing found are of interest to efficient long range hole transfer. From low NRE values especially for the large stacks, see Figure 4 and Table T3, we proposed that the structures of neutral and one-electron oxidized adenine are quite similar and this allows for hole delocalization and ease of hole transfer through stacks of As. The calculated IPs of GG and GGG are lower than all the A-stacks and clearly would act as the hole trap as experiments have shown. In comparison to A-stack, GG and GGG have larger nuclear reorganization energies, NRE, of ~0.5 eV. The large NRE value results from a larger structural change on one-electron oxidiation of GG and GGG stacks which localizes the hole on one base.

IR and Raman spectroscopies are excellent tools for characterization of molecular structure and have been increasingly employed for identification of radical species.[54] Our calculated IR spectra of adenine and A_2 and their radical cations allow us to predict that the presence of adenine radical dimer cation in the A-stacks may be verified by IR. The IR spectra of $A_2^{\bullet+}$ has intense peaks between 1000 – 1600 cm^{-1} which are not present in the corresponding neutral A_2 stack. $A_2^{\bullet+}$ has most intense peak located at ~1100 cm^{-1} which characterizes the presence of adenine dimer radical cation in the large stack. We look forward to experiments which will test this prediction.

Supplementary Material

Refer to Web version on PubMed Central for supplementary material.

Acknowledgments

This work was supported by the NIH NCI under Grant No. R01CA045424 and computational studies were supported by a computational facilities grant NSF CHE-0722689.

References

1. (a) Muller-Dethlefs K, Hobza P. Chem Rev. 2000; 100:143. [PubMed: 11749236] (c) Bendova L, Jurecka P, Hobza P, Vondrasek J. J Phys Chem B. 2007; 111:9975. [PubMed: 17672495] (d) Vondrasek J, Bendova L, Klusak V, Hobza P. J Am Chem Soc. 2005; 127:2615. [PubMed: 15725017] (e) Hobza P, Sponer J. Chem Rev. 1999; 99:3247. [PubMed: 11749516] (f) Kabelac M, Valdes H, Sherer EC, Cramer CJ, Hobza P. Phys Chem Chem Phys. 2007; 9:5000. [PubMed: 17851596] (g) Sponer J, Jurecka P, Marchan I, Luque FJ, Orozco M, Hobza P. Chem Eur J. 2006; 12:2854.(h) Rezac J, Hobza P. Chem Eur J. 2007; 13:2983.(i) Zierkiewicz W, Komorowski L, Michalska D, Cerny J, Hobza P. J Phys Chem B. 2008; 112:16734. [PubMed: 19367910] (j) Wang S, Schaefer HF. J Chem Phys. 2006; 124:044303. [PubMed: 16460158]
2. Kim KS, Tarakeshwar P, Lee JY. Chem Rev. 2000; 100:4145. [PubMed: 11749343]
3. Langner KM, Sokalski WA, Leszczynski J. J Chem Phys. 2007; 127:111102. [PubMed: 17887817]

4. (a) Antony J, Grimme S. Phys Chem Chem Phys. 2006; 8:5287. [PubMed: 19810407] (b) Grimme S. Angew Chem Int Ed. 2008; 47:3430.
5. Hobza P. Phys Chem Chem Phys. 2008; 10:2581. [PubMed: 18464972]
6. (a) Zhao Y, Truhlar DG. Acc Chem Res. 2008; 41:157. [PubMed: 18186612] and refs. therein. (b) Zhao Y, Truhlar DG. J Chem Theory Comput. 2007; 3:289.(c) Cramer CJ, Truhlar DG. Phys Chem Chem Phys. 2009; 11:10757. [PubMed: 19924312] and refs. therein. (d) Jacquemin D, Perpète EA, Ciofini I, Adamo C, Valero R, Zhao Y, Truhlar DG. J Chem Theory Comput. 2010; 6:2071.(e) Zhao Y, Truhlar DG. J Phys Chem A. 2008; 112:1095. [PubMed: 18211046] (f) Valero R, Gomes JRB, Truhlar DG, Illas F. J Chem Phys. 2008; 129:124710. [PubMed: 19045051]
7. (a) Improta R. Phys Chem Chem Phys. 2008; 10:2656. [PubMed: 18464980] (b) Santoro F, Barone V, Improta R. J Am Chem Soc. 2009; 131:15232. [PubMed: 19803481] (c) Golubeva AA, Krylov AI. Phys Chem Chem Phys. 2009; 11:1303. [PubMed: 19224030]
8. Lange AW, Herbert JM. J Am Chem Soc. 2009; 131:3913. [PubMed: 19292489]
9. Kumar A, Sevilla MD. Chem Rev. 2010; 110:7002. and refs therein. [PubMed: 20443634]
10. Becker, D.; Adhikary, A.; Sevilla, MD. Charge Migration in DNA. Chakraborty, T., editor. Springer-Verlag; Berlin, Heidelberg: 2007. p. 139-175.
11. Kumar, A.; Sevilla, MD. Radiation Induced Molecular Phenomena in Nucleic Acids. In: Shukla, MK.; Leszczynski, J.; Leszczynski, J., editors. Challenges and Advances in Computational Chemistry and Physics. Vol. 5. Springer Science + Business Media B.V; Dordrecht, The Netherlands: 2008. p. 577-617.
12. Kumar, A.; Sevilla, MD. Radical and Radical Ion Reactivity in Nucleic Acid Chemistry. Greenberg, M., editor. John Wiley & Sons, Inc; New York: 2010. p. 1-40.
13. Becker, D.; Sevilla, MD. Electron Paramagnetic Resonance. In: Gilbert, BC.; Davies, MJ.; Murphy, DM., editors. Royal Society of Chemistry Specialist Periodical Report. Vol. 21. Royal Society of Chemistry; London: 2008. p. 33
14. Steenken S. Chem ReV. 1989; 89:503.
15. Boon EM, Livingston AL, Chmiel NH, David SS, Barton JK. Proc Natl Acad Sci USA. 2003; 100:12543. [PubMed: 14559969]
16. DeRosa MC, Sancar A, Barton JK. Proc Natl Acad Sci USA. 2005; 102:10788. [PubMed: 16043698]
17. Boon EM, Ceres DM, Drummond TG, Hill MG, Barton JK. Nat Biotechnol. 2000; 18:1096. [PubMed: 11017050]
18. Okamoto A, Tanaka K, Saito I. J Am Chem Soc. 2004; 126:9458. [PubMed: 15281839]
19. (a) Gorodetsky AA, Buzzeo MC, Barton JK. Bioconjugate Chem. 2008; 19:2285.(b) Genereux JC, Barton JK. Chem Rev. 2010; 110:1642. [PubMed: 20214403] (c) Shao F, O'Neill MA, Barton JK. Proc Natl Acad Sci USA. 2004; 101:17914. [PubMed: 15604138]
20. Schuster, GB., editor. Long-Range Charge Transfer in DNA, I and II. Vol. 236 and 237. Springer; New York: 2004.
21. Wagenknecht, HA., editor. Charge Transfer in DNA. Wiley-VCH; Weinheim, Germany: 2005.
22. Grozema FC, Berlin YA, Siebbeles LDA. J Am Chem Soc. 2000; 122:10903.
23. Takada T, Kawai K, Fujitsuka M, Majima T. Proc Natl Acad Sci USA. 2004; 101:14002. [PubMed: 15381780]
24. Osakada Y, Kawai K, Fujitsuka M, Majima T. Chem Commun. 2008; 23:2656.
25. (a) Voityuk AA, Siriwong K, Rösch N. Angew Chem Int Ed. 2004; 43:624.(b) Sadowska-Aleksiejew A, Rak J, Voityuk AA. Chem Phys Lett. 2006; 429:546.(c) Voityuk AA, Rösch N, Bixon M, Jortner J. J Phys Chem B. 2000; 104:9740.
26. (a) Barnett RN, Cleveland CL, Joy A, Landman U, Schuster GB. Science. 2001; 294:567. [PubMed: 11641491] (b) Schuster GB. Acc Chem Res. 2000; 33:253. [PubMed: 10775318]
27. Shimazaki T, Asai Y, Yamashita K. J Phys Chem B. 2005; 109:1295. [PubMed: 16851094]
28. (a) Lewis JP, Cheatham TE, Starikov EB, Wang H, Sankey OF. J Phys Chem B. 2003; 107:2581. (b) Kubar T, Elstner M. J Phys Chem B. 2009; 113:5653. [PubMed: 19331336] (c) Steinbrecher T, Koslowski T, Case DA. J Phys Chem B. 2008; 112:16935. [PubMed: 19049302] (d) Kurnikov IV, Tong GSM, Madrid M, Beratan DN. J Phys Chem B. 2002; 106:7.

29. (a) Conwell EM. Proc Natl Acad Sci USA. 2005; 102:8795. [PubMed: 15956188] (b) Conwell EM, Basko DM. J Am Chem Soc. 2001; 123:11441. [PubMed: 11707121]
30. (a) Giese B, Amaudrut, Köhler A-K, Sporman M, Wessely S. Nature. 2001; 412:318. [PubMed: 11460159] (b) Giese B. Acc Chem Res. 2000; 33:631–636. [PubMed: 10995201]
31. (a) Buchvarov I, Wang Q, Raytchev M, Trifonov A, Fiebig T. Proc Natl Acad Sci USA. 2007; 104:4794. [PubMed: 17360401] (b) Fiebig T. J Phys Chem B. 2009; 113:9348. [PubMed: 19534481]
32. Tonzani S, Schatz GC. J Am Chem Soc. 2008; 130:7607. [PubMed: 18491899]
33. (a) Kumar A, Sevilla MD. J Phys Chem B. 2006; 110:24181. [PubMed: 17125390] (b) Blancafort L, Voityuk AA. J Phys Chem A. 2006; 110:6426. [PubMed: 16706397] (c) Voityuk AA. J Phys Chem B. 2005; 109:10793. [PubMed: 16852312]
34. Adhikary A, Kumar A, Khanduri D, Sevilla MD. J Am Chem Soc. 2008; 130:10282. [PubMed: 18611019]
35. Fujitsuka M, Tojo S, Shibahara M, Watanabe M, Shinmyozu T, Majima TJ. Phys Chem A. 10.1021/jp110916m
36. (a) Adhikary A, Khanduri D, Sevilla MD. J Am Chem Soc. 2009; 131:8614. [PubMed: 19469533] (b) Lewis FD, Letsinger RL, Wasielewski MR. Acc Chem Res. 2001; 34:159. [PubMed: 11263874]
37. SPARTAN, version 50. Wavefunction, Inc; Irvine, CA: 1997.
38. Frisch, MJ.; Trucks, GW.; Schlegel, HB.; Scuseria, GE.; Robb, MA.; Cheeseman, JR.; Scalmani, G.; Barone, V.; Mennucci, B.; Petersson, GA.; Nakatsuji, H.; Caricato, M.; Li, X.; Hratchian, HP.; Izmaylov, AF.; Bloino, J.; Zheng, G.; Sonnenberg, JL.; Hada, M.; Ehara, M.; Toyota, K.; Fukuda, R.; Hasegawa, J.; Ishida, M.; Nakajima, T.; Honda, Y.; Kitao, O.; Nakai, H.; Vreven, T.; Montgomery, JA., Jr; Peralta, JE.; Ogliaro, F.; Bearpark, M.; Heyd, JJ.; Brothers, E.; Kudin, KN.; Staroverov, VN.; Kobayashi, R.; Normand, J.; Raghavachari, K.; Rendell, A.; Burant, JC.; Iyengar, SS.; Tomasi, J.; Cossi, M.; Rega, N.; Millam, JM.; Klene, M.; Knox, JE.; Cross, JB.; Bakken, V.; Adamo, C.; Jaramillo, J.; Gomperts, R.; Stratmann, RE.; Yazyev, O.; Austin, AJ.; Cammi, R.; Pomelli, C.; Ochterski, JW.; Martin, RL.; Morokuma, K.; Zakrzewski, VG.; Voth, GA.; Salvador, P.; Dannenberg, JJ.; Dapprich, S.; Daniels, AD.; Farkas, O.; Foresman, JB.; Ortiz, JV.; Cioslowski, J.; Fox, DJ. Gaussian 09. Gaussian, Inc; Wallingford CT: 2009.
39. (a) GaussView. Gaussian, Inc; Pittsburgh, PA: 2003. (b) Allouche, AR. Gabedit is a free Graphical User Interface for computational chemistry packages. It is available from http://gabedit.sourceforge.net/
40. Close DM. J Phys Chem A. 2010; 114:1860. [PubMed: 20050713]
41. Mantz YA, Gervasio FL, Laino T, Parrinello M. J Phys Chem A. 2007; 111:105. [PubMed: 17201393]
42. VandeVondele J, Sprik M. Phys Chem Chem Phys. 2005; 7:1363. [PubMed: 19787955]
43. (a) Guidon M, Hutter J, VandeVondele J. J Chem Theory Comput. 2010; 6:2348–2364.(b) Korth M, Grimme S. J Chem Theory Comput. 2009; 5:993.(c) Goerigk L, Grimme SJ. Chem Theory Comput. 10.1021/ct100466k(d) Henderson TM, Izmaylov AF, Scalmani G, Scuseria GE. J Chem Phys. 2009; 131:044108. [PubMed: 19655838]
44. Hohenstein EG, Chill ST, Sherrill CD. J Chem Theory Comput. 2008; 4:1996.
45. Gu JD, Wang J, Leszczynski J, Xie YM, Schaefer HF. Chem Phys Lett. 2008; 458:164.
46. Drew HR, Wing RM, Takano T, Broka C, Tanaka S, Itakura K, Dickerson RE. Proc Natl Acad Sci USA. 1981; 78:2179. [PubMed: 6941276]
47. MacDonald D, Herbert K, Zhang X, Polgruto T, Lu P. J Mol Biol. 2001; 306:1081. [PubMed: 11237619]
48. Bravaya KB, Kostko O, Ahmed M, Krylov AI. Phys Chem Chem Phys. 2010; 12:2292. [PubMed: 20449342]
49. Dreuw A, Starcke JH, Wachtveitl J. Chemical Physics. 2010; 373:2.
50. Saito I, Takayama M, Sugiyama H, Nakatani K, Tsuchida A, Yamamoto M. J Am Chem Soc. 1995; 117:6406.
51. Hall DB, Holmlin RE, Barton JK. Nature. 1996; 382:731. [PubMed: 8751447]

52. Adhikary A, Kumar A, Becker D, Sevilla MD. J Phys Chem B. 2006; 110:24171. [PubMed: 17125389]

53. (a) Hush NS, Cheung AS. Chem Phys Lett. 1975; 34:11.(b) Orlov VM, Smirnov AN, Varshavsky YM. Tetrahedron Lett. 1976; 17:4315.(c) Li X, Cai Z, Sevilla MD. J Phys Chem A. 2002; 106:9345.(d) Li X, Cai Z, Sevilla MD. J Phys Chem B. 2001; 105:10115.(e) Olofsson J, Larsson S. J Phys Chem B. 2001; 105:10398.(f) Priyadarshy S, Risser SM, Beratan DN. J Phys Chem. 1996; 100:17678.(g) Berashevich JA, Chakraborty T. Chem Phys Lett. 2007; 446:159.

54. (a) Parker AW, Lin CY, George MW, Towrie M, Kuimova MK. J Phys Chem B. 2010; 114:3660. [PubMed: 20175506] (b) Kuimova MK, Gill PMW, Lin C-Y, Matousek P, Towrie M, Sun XZ, George MW, Parker AW. Phys Chem Chem Phys. 2007; 6:949.(c) Tripathi GNR. J Phys Chem A. 2004; 108:5139.(d) Tripathi GNR, Su Y, Bentley J, Fessenden RW, Jiang PY. J Am Chem Soc. 1996; 118:2245.(e) Tripathi GNR. J Am Chem Soc. 2003; 125:1178. [PubMed: 12553814] (f) Tripathi, GNR. Advances in Spectroscopy: Time-Resolved Spectroscopy. Clark, RJH.; Hester, RE., editors. Vol. 18. John Wiley & Sons; New York: 1989. p. 157-218.(g) Nir E, Kleinermanns K, de Vries MS. Nature. 2000; 408:949. [PubMed: 11140676]

55. Smith QA, Gordon MS. J Phys Chem A. 201110.1021/jp109983x

56. Shao F, Augustyn K, Barton JK. J Am Chem Soc. 2005; 127:17445. [PubMed: 16332096]

57. Henderson PT, Jones D, Hampikian G, Kan YZ, Schuster GB. Proc Natl Acad Sci USA. 1999; 96:8353. [PubMed: 10411879]

58. Conwell EM, Rakhmanova SV. Proc Natl Acad Sci USA. 2000; 97:4556. [PubMed: 10758150]

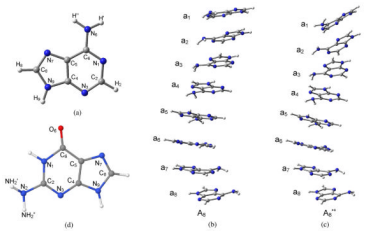

Figure 1.
(a) Atom numbering scheme of adenine base present in A-stacks. M06-2X/6-31G* optimized structure of A_8 in (b) neutral and (c) radical cation states. Adenine bases present in the stack are numbered as a_i (i = 1 – 8). (d) Atom numbering scheme of guanine base present in G-stacks.

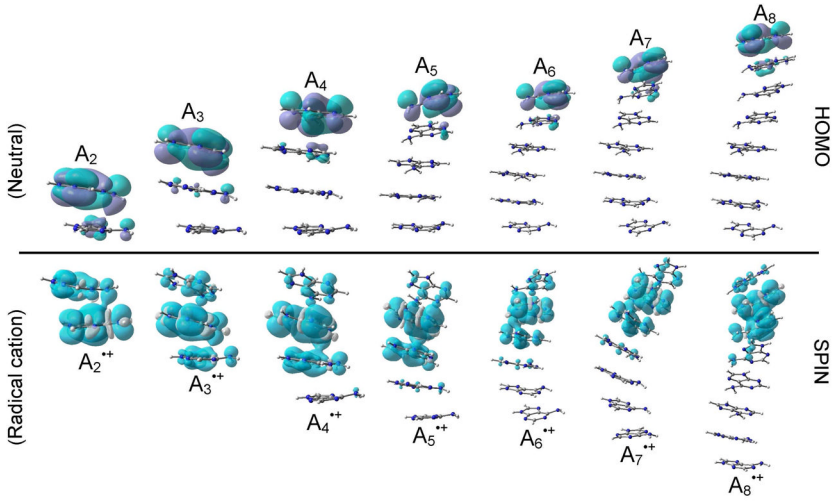

Figure 2.

Plots of highest occupied molecular orbital (HOMO) in optimized neutral adenine stacks A_i (i = 1 – 8) (above the line) and spin density distributions in the optimized radical cation (one-electron oxidation) adenine stacks $A_i^{\bullet+}$ (i = 1 – 8) (below the line The HOMOs and spin density distributions in the plots were calculated using the M06-2X/6-31G* method.

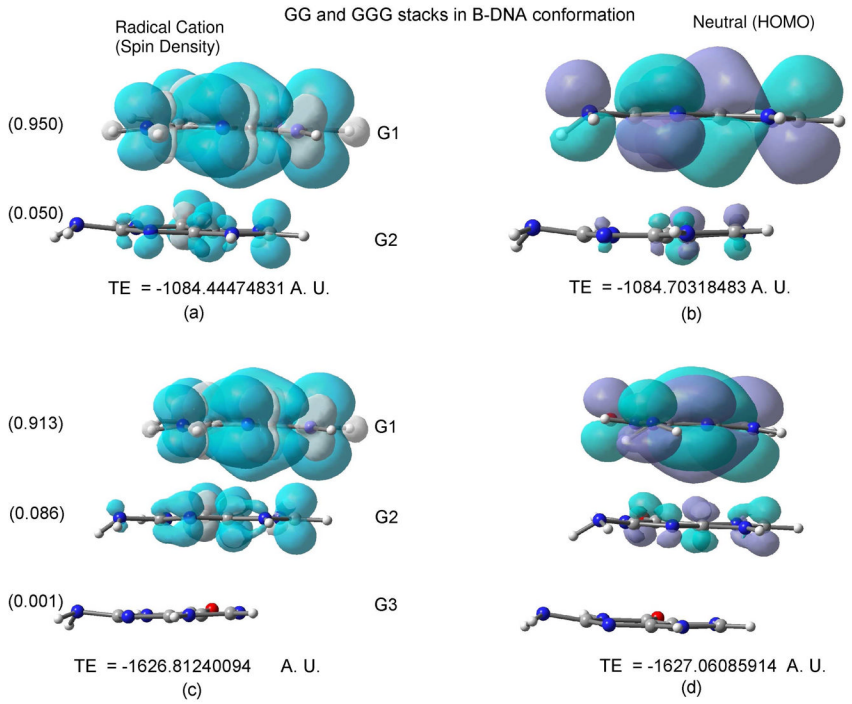

Figure 3.

Spin density and HOMO plots of GG and GGG stacks in radical cation (a, c) and neutral states (b, d). The geometries were optimized using M06-2X/6-31G* method. Structures were optimized in B-DNA conformation by relaxing the inter-base distances. Mulliken spin densities on each G base in the stack is shown in parentheses.

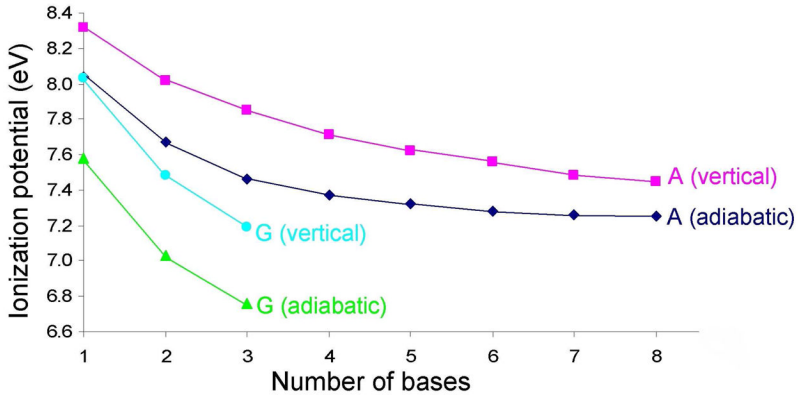

Figure 4.
M06-2X/6-31G* calculated vertical and adiabatic ionization potentials (eV) of adenine and guanine stacks.

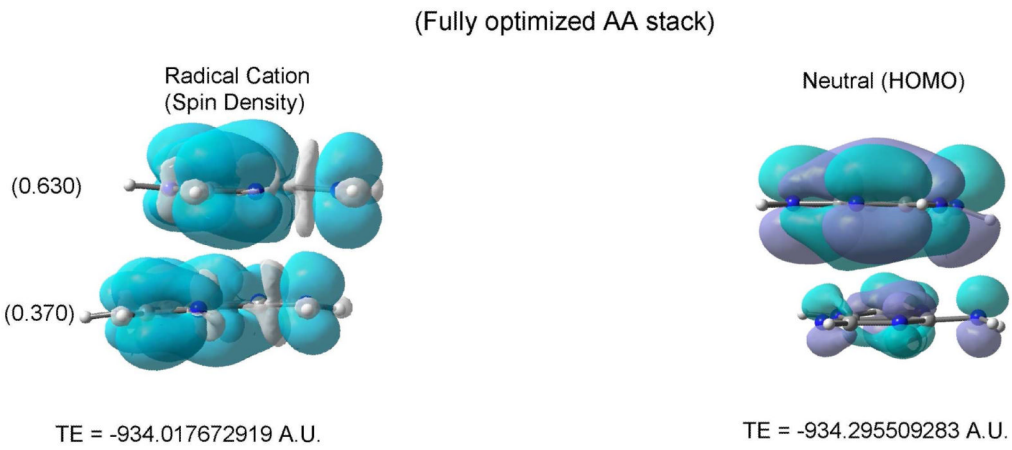

Figure 5.
Spin density and HOMO plots of A_2 stack in radical cation (a) and neutral (b) states. The geometries were fully optimized using M06-2X/6-31G* method.

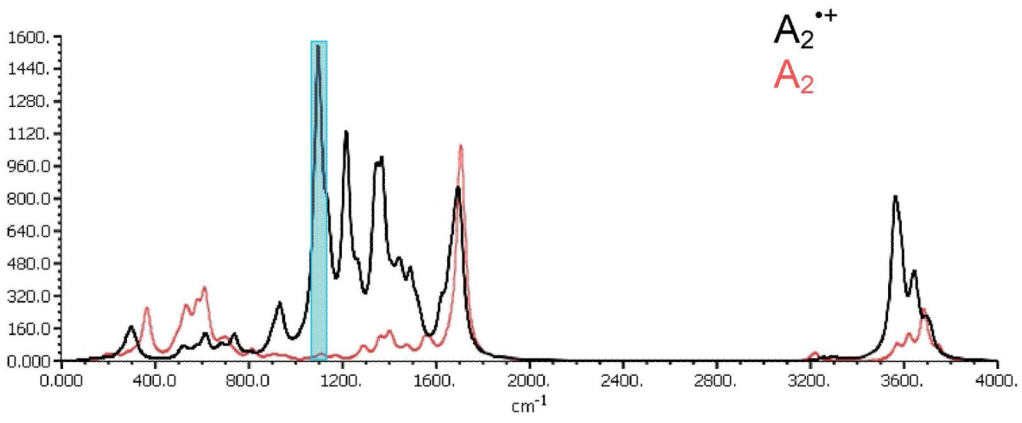

Figure 6.

M06-2X/6-31G* calculated vibrational spectra of A_2 and $A_2^{\bullet+}$. The spectra of $A_2^{\bullet+}$ has an intense peak at ~1100 cm^{-1}, shown by light blue rectangle. **Structure is fully optimized** at M06-2X/6-31G* level of theory as shown in Figure 5.

Table 1

Inter-atomic distance (Å) in neutral and radical cation states of A_8. The distances were calculated between two consecutive bases. The geometry is fully optimized in the B-DNA conformation using M06-2X/6-31G* method.

Distance[b] (Å)	**Neutral[a]**									
	N_1	**C_2**	**N_3**	**C_4**	**C_5**	**C_6**	**N_7**	**C_8**	**N_9**	**N_6**
a_1–a_2	3.21	3.44	3.73	3.74	3.56	3.25	3.89	4.20	4.16	3.26
a_2–a_3	3.18	3.42	3.71	3.72	3.53	3.23	3.89	4.23	4.17	3.27
a_3–a_4	3.17	3.41	3.70	3.72	3.53	3.22	3.90	4.25	4.18	3.26
a_4–a_5	3.18	3.43	3.73	3.74	3.55	3.24	3.90	4.23	4.17	3.26
a_5–a_6	3.18	3.42	3.71	3.72	3.53	3.23	3.90	4.23	4.17	3.25
a_6–a_7	3.18	3.42	3.73	3.74	3.55	3.24	3.90	4.23	4.17	3.26
a_7–a_8	3.21	3.44	3.74	3.75	3.56	3.26	3.91	4.22	4.17	3.29
Average	3.19	3.43	3.72	3.73	3.54	3.24	3.90	4.23	4.17	3.26
Average[c]	3.32	3.68	3.98	3.88	3.54	3.23	3.87	4.30	4.36	3.18
	Radical cation[a]									
	N_1	C_2	N_3	C_4	C_5	C_6	N_7	C_8	N_9	N_6
a_1–a_2	3.17	3.42	3.70	3.72	3.54	3.23	3.85	**4.14**	4.12	**3.18**
a_2–a_3	**3.08**	**3.30**	**3.63**	**3.65**	**3.45**	3.18	**3.79**	**4.13**	**4.07**	3.25
a_3–a_4	3.13	3.37	3.70	3.73	3.52	3.21	3.87	4.22	4.16	3.27
a_4–a_5	3.16	3.40	3.72	3.75	3.55	3.24	3.92	4.25	4.19	3.28
a_5–a_6	3.17	3.40	3.72	3.75	3.56	3.24	3.92	4.25	4.19	3.28
a_6–a_7	3.18	3.42	3.73	3.75	3.56	3.25	3.92	4.24	4.19	3.29
a_7–a_8	3.19	3.43	3.75	3.77	3.58	3.27	3.93	4.25	4.20	3.30
Average	3.15	3.39	3.71	3.73	3.54	3.23	3.89	4.21	4.16	3.26

[a] For atom numbering, see Figure 1a.

[b] Inter-atomic distance calculated between the corresponding atoms of the two consecutive stacked adenine bases in the stack. For numbering of the individual adenine base (a_i; i = 1 – 8) present in the stack, see Figure 1.

[c] NMR solution structure of the DNA dodecamer GGCAAAAAACGG, see Ref. 47.

Table 2

M06-2X/6-31G* calculated Mulliken charges and spin density distribution on each adenine base in the neutral and radical cation stack.

Stack	State	Total charge on each adenine base in the stack[a]							
		5′-A_i-3′ (i = 2 – 8)[b]							
		a_1	**a_2**	**a_3**	**a_4**	**a_5**	**a_6**	**a_7**	**a_8**
A_2	Cation	0.190	0.810						
	Neutral	−.011	0.011						
	Difference[c]	**0.201**	**0.799**						
	Spin[d]	0.164	0.836						
A_3	Cation	0.096	0.783	0.121					
	Neutral	−.011	−.004	0.015					
	Difference[c]	**0.107**	**0.787**	**0.106**					
	Spin[d]	0.069	0.848	0.083					
A_4	Cation	0.074	0.756	0.125	0.045				
	Neutral	−.010	−.003	−.003	0.016				
	Difference[c]	**0.084**	**0.759**	**0.128**	**0.029**				
	Spin[d]	0.048	0.820	0.125	0.007				
A_5	Cation	0.066	0.740	0.145	0.020	0.029			
	Neutral	−.010	−.004	−.0	−.001	0.016			
	Difference[c]	**0.076**	**0.744**	**0.145**	**0.021**	**0.013**			
	Spin[d]	0.040	0.801	0.149	0.010	0.0			
A_6	Cation	0.064	0.725	0.158	0.022	0.007	0.024		
	Neutral	−.011	−.002	0.0	−.004	0.0	0.034		
	Difference[c]	**0.075**	**0.727**	**0.158**	**0.026**	**0.007**	**−.010**		
	Spin[d]	0.038	0.785	0.164	0.013	0.001	0.0		
A_7	Cation	0.059	0.704	0.179	0.026	0.007	0.004	0.021	
	Neutral	−.010	−.005	−.0	−.002	0.0	0.0	0.016	

Stack	State	Total charge on each adenine base in the stack[a]							
		5′-A_i-3′ (i = 2 – 8)[b]							
		a_1	**a_2**	**a_3**	**a_4**	**a_5**	**a_6**	**a_7**	**a_8**
A_8	Difference[c]	**0.069**	**0.709**	**0.179**	**0.028**	**0.007**	**0.004**	**0.005**	
	Spin[d]	0.034	0.760	0.187	0.017	0.001	0.0	0.0	
	Cation	0.055	0.669	0.213	0.030	0.007	0.003	0.003	0.020
	Neutral	−.011	−.002	0.0	−.003	0.0	−.002	0.001	0.017
	Difference[c]	**0.066**	**0.671**	**0.213**	**0.033**	**0.007**	**0.005**	**0.002**	**0.003**
	Spin[d]	0.032	0.721	0.225	0.022	0.001	0.0	0.0	0.0

[a] Mulliken charge analysis.

[b] See Figure 1b, c for numbering of adenine bases in the stack.

[c] Difference = Difference between the total charge on adenine base in their cation radical and neutral states.

[d] Mulliken spin densities on each adenine base in the stack.

Table 3

Calculated and experimental isotropic hyperfine coupling constants (HFCCs) in MHz for radical cation of G, GG and GGG.

	M06-2X/6-31G*								
		GG[b]		GGG[c]					
Atom[a]	G	G1	G2	G1	G2	G3	GG[d] (QCISD/3-21G)	Exp.[e] ($G^{\bullet+}$)	Exp.[f] ($G^{\bullet+}$)
N_1	−3.17	−2.93	−0.02	−2.83	−0.12	−0.01	−3.76	-	-
N_3	15.68	14.88	0.49	14.98	0.86	−0.01	18.87	12.1	16.8
N_7	−2.78	−2.87	0.04	−2.61	−0.13	0.03	−8.74	-	-
N_9	−6.75	−6.35	−0.09	−5.82	−0.33	0.01	−8.02	-	-
N_2	8.01	7.69	−0.06	7.64	0.13	0.00	5.86	6.1	10.0
C_8-H	−22.43	−20.84	−1.25	−19.63	−2.05	−0.04	−30.07	−21	−14.5
NH_2'[g]	−9.30	−8.03	0.05	−7.48	0.12	0.00	−7.10	-	−12.1
NH_2''[g]	−8.36	−6.99	−0.07	−6.35	−0.14	0.000	−7.89	-	−12.1

[a] See Figure 1(d) for numbering.

[b] See Figure 3(a) for base numbering in GG.

[c] See Figure 3(c) for base numbering in GGG.

[d] From Ref. 40. Couplings localized on one G in GG stack are given in Ref. 40.

[e] ESR experiment for 2'deoxyguanosine in D_2O from Ref. 52

[f] Experimental result from Ref. 40. HFCCs values for guanine cation radical from single crystal ESR experiment.

[g] NH_2 proton coupling.